

Bifurcations in Boltzmann-Langevin One Body dynamics for fermionic systems

P.Napolitani^a, M.Colonna^b

^aIPN, CNRS/IN2P3, Université Paris-Sud 11, 91406 Orsay cedex, France

^bINFN-LNS, Laboratori Nazionali del Sud, 95123 Catania, Italy

Abstract

We investigate the occurrence of bifurcations in the dynamical trajectories depicting central nuclear collisions at Fermi energies. The quantitative description of the reaction dynamics is obtained within a new transport model, based on the solution of the Boltzmann-Langevin equation in three dimensions, with a broad applicability for dissipative fermionic dynamics.

Dilute systems formed in central collisions are shown to fluctuate between two energetically favourable mechanisms: reverting to a compact shape or rather disintegrating into several fragments. The latter result can be connected to the recent observation of bimodal distributions for quantities characterising fragmentation processes and may suggest new investigations.

1. Introduction

Phase transitions are general phenomena occurring in interacting many-body systems [1, 2, 3, 4]. Over the past years, many efforts have been devoted to the identification of new features related to finite-size effects. As shown by recent thermodynamical analyses, first-order phase transitions in finite systems are characterised by negative specific heat and bimodal behaviour of the distribution of the order parameter [5, 6]. The latter physically corresponds to the simultaneous presence of different classes of physical states for the same value of the system conditions that trigger the transition (like the temperature, for instance).

In particular, the appearance of phase transitions from the liquid to the vapour phases has been widely investigated in the context of the nuclear multifragmentation phenomenon [7, 8, 4, 9]. Indeed, due to the analogies between the nuclear forces and the Van-der-Waals interaction, the nuclear matter equation of state (EOS) foresees such a possibility [10, 11]. The theoretical findings cited above have stimulated corresponding thermodynamical analyses of the properties of the products issued from nuclear reactions at Fermi energies. Under suitable conditions, a bimodal character of experimental observables, such as the size of the heaviest cluster produced in each collision event [12], or the asymmetry between the charges of the two heaviest reaction products [13] has been revealed. Many investigations have also been focused on the complex nuclear many-body dynamics, to probe the reaction mechanisms governing the occurrence of phase transitions [14, 15, 16, 17]. Within such a context, nuclear fragmentation studies at intermediate energies (above 50 MeV per nucleon) have recently pointed out that bimodality could have a dynamical origin, related to the fragment-formation mechanism [18], without necessarily requiring the reaching of thermodynamical equilibrium.

From a general point of view, interacting many-body systems may experience a very rich dynamics, ranging from mechanisms dominated by one-body (mean-field) effects to phenom-

ena governed by strong fluctuations and correlations. In the regime of low-energy collective processes, nuclear dynamics presents a rather stable character; this is the domain where the fluctuation mechanism can be described in the small amplitude limit, restricting to mean-field (quantum) fluctuations of collective observables [19, 20]. This limit is exceeded when violent perturbations, like for instance dissipative heavy-ion collisions, bring the system beyond the one-body collective dynamics, with two-body nucleon collisions and correlations playing an important role. Along the compression-expansion path traced by the nuclear reaction, fluctuations introduce the anisotropy seeds from which ‘nuclear droplets’ can develop. More precisely, the system may access mechanically unstable regions of the EOS, called spinodal, where a density rise is related to a pressure fall; there, phase-space fluctuations are even amplified, leading to phase separation [17, 8]. As soon as a mottling pattern stands out at low density, i.e. at the boundary of the phase separation, a bundle of bifurcations into a variety of different dynamical paths may set in.

2. The Boltzmann-Langevin-One-Body model

The aim of this work is to further investigate the dynamical trajectory of disassembling nuclear systems, seeking for features associated with phase transitions. In particular, we will explore the possible occurrence of bifurcation patterns and bimodal behaviour in central heavy-ion reactions at beam energies around the multifragmentation threshold.

This study is undertaken in the framework of a new numerical implementation of the Boltzmann-Langevin (BL) equation, well suited to describe out-of-equilibrium processes, such as nuclear collisions: the Boltzmann-Langevin-One-Body (BLOB) model. The BL equation describes the time evolution of the semiclassical one-body distribution function $f(\mathbf{r}, \mathbf{p}, t)$ in response to the mean-field potential, incorporating the effect of fluctuations and correlations due to hard two-body scattering [21, 22, 23, 24].

Hence the distribution function f evolves according to the action of the effective Hamiltonian $H[f]$, the average Boltzmann collision integral $\bar{I}[f]$, and the fluctuating term $\delta I[f]$ as:

$$\dot{f} = \partial_t f - \{H[f], f\} = \bar{I}[f] + \delta I[f]. \quad (1)$$

This form indicates that the residual interaction, represented by the right-hand side of eq. 1, is expressed in terms of the one-body distribution function f .

Like in standard transport approaches [25], we sample the dynamics through the test-particle method, under the assumption of spatial and temporal locality of the two-body collisional process. N_{test} particles per nucleon are employed. The Boltzmann-Langevin theory describes fluctuations of f on a size scale of h^3 , but it leaves the shape of such a phase-space volume arbitrary (see the discussion in ref. [26]). This same arbitrariness characterises other molecular-dynamics or Boltzmann-like approaches. In this respect, we chose to follow the prescription of Bauer and Bertsch [27]: in order to solve the BL equation, they proposed to define nucleon wave packets by organising test particles in phase-space agglomerates of N_{test} elements. However, in ref. [27] Pauli blocking was checked only for the centroids of the nucleon clouds: the effect of such approximation on the fermionic dynamics was analysed in refs. [23, 28], where it was concluded that an incomplete treatment of Pauli blocking affects the mechanism of fluctuation development. The above recommendation was taken into account in ref. [26], in treating the schematic case of nuclear matter in a periodic box: such approach confirmed that an accurate treatment of the Pauli blocking is the key for correctly describing the fluctuation mechanism in full phase space. By further improving the above approach in a full model for heavy-ion collisions, we built a novel numerical procedure where nucleon-nucleon (N-N) correlations are implemented by accurately treating the Pauli-blocking factors of agglomerates of N_{test} elements of identical isospin. This arrangement, which simulates nucleon wave packets, is redefined at successive time steps and locally, for couples of colliding agglomerates. According to this rescaling and for elastic N-N collisions only, the average rate of change of the occupancy f_a around the phase-space location $(\mathbf{r}_a, \mathbf{p}_a)$ at a given time takes the form:

$$\dot{f}_a(\mathbf{r}_a, \mathbf{p}_a) = g \int \frac{d\mathbf{p}_b}{h^3} \int d\Omega W_{(AB \leftrightarrow CD)} F_{(AB \rightarrow CD)}, \quad (2)$$

where g denotes the degeneracy, and integrations are over momenta \mathbf{p}_b and scattering angles Ω . The first integration argument is the symmetric transition rate from an intermediate state AB to a final configuration CD. To select the test particles defining the nucleon wave packets A and B, we adopt the following procedure: We consider a sphere, centred at the position \mathbf{r}_a , with radius equal to the scattering distance, associated with the free elastic N-N cross section at Fermi energies (taken equal to 50 mb); among all test particles inside the sphere, we pick up the N_{test} closest particles to the elements a and b in momentum space, respectively. The final state is represented by $c \in C$ and $d \in D$. The transition rate is obtained by averaging over all couples of test particles involved in the transition $\Sigma = (AB \rightarrow CD)$,

in terms of relative velocity and differential N-N cross section:

$$W_{(AB \leftrightarrow CD)} = \left\langle |v_a - v_b| \frac{d\sigma}{d\Omega} \right\rangle_{\Sigma} = \left\langle W_{(ab \leftrightarrow cd)} \right\rangle_{\Sigma}. \quad (3)$$

The second integration argument contains the product of occupancies of the entire agglomerates $f_{A \dots D}$ and of the associated vacancies $\bar{f}_{A \dots D}$:

$$F_{(AB \rightarrow CD)} = \bar{f}_A \bar{f}_B f_C f_D - f_A f_B \bar{f}_C \bar{f}_D = \left\langle F_{(ab \rightarrow cd)} \right\rangle_{\Sigma}. \quad (4)$$

Rewritten in terms of test-particles, the representation of eq. 4 indicates that only the fraction of the packets which are really modified by the scattering can significantly contribute to the transition probability, while overlapping volumes contribute to the Pauli-blocking factors.

On this basis, full phase-space fluctuations are introduced in the equation of motion by moving simultaneously the test-particle agglomerates, in analogy with the extended-TDHF procedure of including perturbations in the Slater configuration [29]. The scattering is decided by confronting the probability $W \times F$ with a random number and scanning the entire phase space in search of collision configurations at successive time steps. Since all test particles belonging to the agglomerates A and B can be reconsidered as starting points of new collision processes, the scattering probability has to be suitably rescaled, dividing it by N_{test}^2 . Once the sorting allows for a scattering to occur, modulation functions are applied to precisely adapt the density profile of final-states to the available vacancy profile $\bar{f}_{A \dots D}$, with the requirement of imposing the most compact configuration compatible with the constraint of energy conservation [30]; the resulting occupation functions of the modulated final-state density profiles $(f_{A \dots D})_M$ should approach unity.

The extension of the wave packets makes necessary to pay special attention to scatterings close to the surface of the system, i.e. occurring across potential boundaries: confronting the shape of the wave packet to the shape of the surface, the blocking factors are increased in proportion to the spread of the nucleon packet outside of the boundary (similarly to what is done in some molecular-dynamics approaches [14]).

It occurs in some situations, for instance when low densities are attained, that the nuclear system is brought to explore regions of the phase diagram where it becomes unstable against density fluctuations, like the spinodal region. The action of the BL term results in agitating the density profile over several wave lengths. It can be proven for the proposed BL approach (through an analysis of the linear response in the mean field, see refs. [31, 17]) that the amplitude of the unstable modes grows according to the specific dispersion relation associated with the employed mean-field interaction.

3. Application to head-on heavy-ion collisions at Fermi energies

In the following, the BLOB model is applied to a highly constraining phenomenology: the low-energy threshold for multi-fragmentation in head-on heavy-ion collisions at Fermi energies. We will also refer to results of the so-called Stochastic

Mean Field (SMF) model [24, 17], that corresponds to an approximate treatment of the BL equation. In SMF, fluctuations are projected on the coordinate space and injected by agitating the spatial density profile. We will show that the implementation of fluctuations in full phase space (as in BLOB) improves significantly the reaction dynamics.

Like in ref. [32], for the simulation we use a soft equation of state with $k_{\text{inf}} = 200$ MeV; the potential component of the symmetry energy of the EOS is given by a linear term as a function of the density (asy-stiff). For numeric purposes, the transition rate has been rewritten as $W \approx \langle |v_a - v_b| \rangle \Sigma (d\sigma_s/d\Omega)$ by introducing a screened in-medium cross section σ_s (from ref. [33]), corresponding to the transition $(AB \leftrightarrow CD)$.

Fig. 1 illustrates a study of the N-N collision statistics for the collision $^{136}\text{Xe} + ^{124}\text{Sn}$ at 32 AMeV, at a central impact parameter ($b = 0$). The number of events considered is 600. Only a tiny fraction of the attempted N-N collisions is permitted by Pauli-blocking factors. Indeed the Pauli-blocking rejection rate R_p , defined as the ratio between rejected and attempted collisions, is close to unity. The average number of effective N-N collisions $\langle N_{\text{eff}} \rangle$ reflects the average density evolution of the system: a maximum is encountered in correspondence with the largest compression and a minimum marks the subsequent expansion mechanism. This evolution is illustrated for one single event in the lower band of fig. 1. Later on, $\langle N_{\text{eff}} \rangle$ increases again indicating that the process of fragment formation sets in, and it finally levels off till, around 300 fm/c, the system has stabilised into a well defined configuration. Thus fragments are formed when the system expands, according to the spinodal decomposition scenario [17]. The equality between the mean value and the variance ensures that Langevin fluctuations stand out with the correct amplitude [26]. Some examples of fragmentation patterns appearing at 300 fm/c for the same initial conditions are collected in the right band of the figure; their variety already

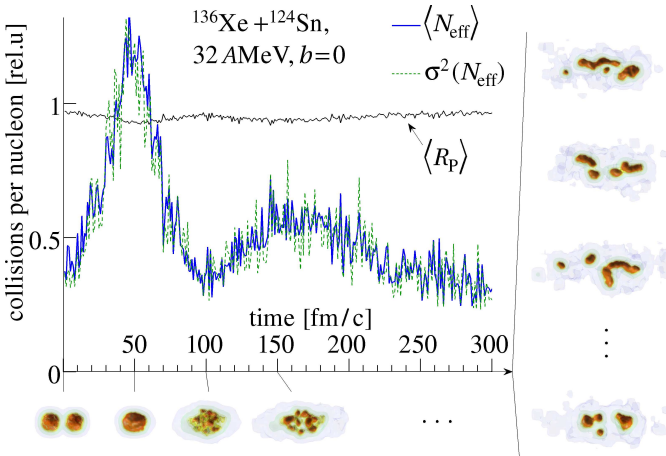


Figure 1: (Color online) N-N collisions in $^{136}\text{Xe} + ^{124}\text{Sn}$ at 32 AMeV for $b = 0$: mean Pauli-blocking rejection rate $\langle R_p \rangle$, and mean evolution of the number of effective collisions $\langle N_{\text{eff}} \rangle$ which equals its variance $\sigma^2(N_{\text{eff}})$. Bottom: Time evolution of the projected density profile. Right band: For the same initial conditions, bifurcations lead to several different fragmentation patterns at 300 fm/c.

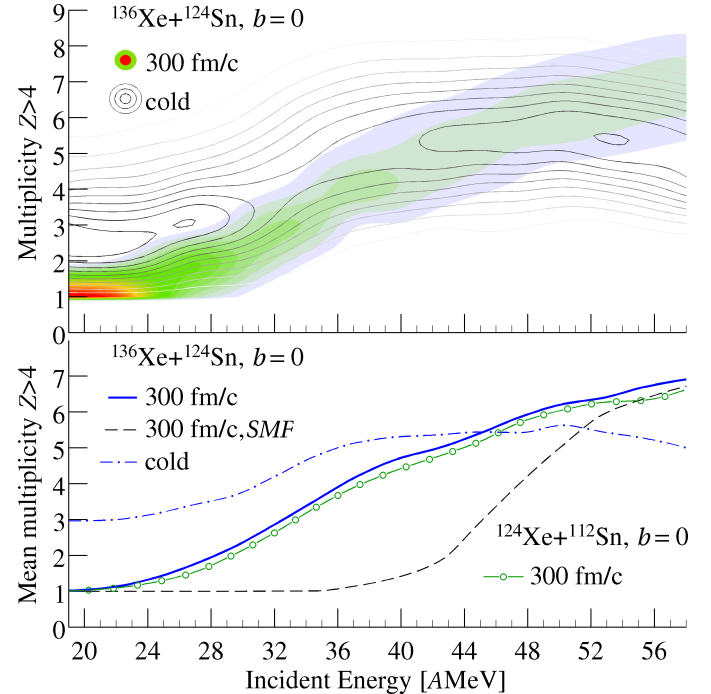


Figure 2: (Color online) Top. Multiplicity distribution of fragments with $Z > 4$ as a function of the incident energy in $^{136}\text{Xe} + ^{124}\text{Sn}$ ($b = 0$) at 300 fm/c (filled contours) and after secondary decay (contour lines). Bottom. Corresponding mean values; additional calculation for the system $^{124}\text{Xe} + ^{112}\text{Sn}$ is also shown. The heaviest system is also simulated within the SMF approach.

signs the presence of bifurcations.

3.1. Onset of fragmentation

Having verified that Langevin fluctuations show up with the expected properties, we let vary the incident energy over a large interval, from 19 to 58 AMeV. The corresponding evolution of the fragment multiplicity, calculated by counting all fragments with charge number¹ $Z > 4$ standing out at 300 fm/c, is shown in fig. 2. The general behaviour that BLOB traces is that a transition from incomplete fusion (just one nucleus observed) to multifragmentation occurs between 20 and 30 AMeV in $^{136}\text{Xe} + ^{124}\text{Sn}$. The less neutron rich system $^{124}\text{Xe} + ^{112}\text{Sn}$, also simulated, presents the same evolution, but retarded with a shift of about 2 AMeV to larger bombarding energies. Indeed the corresponding IMF multiplicity is smaller, in agreement with experimental findings [34]. The same observable is also deduced at asymptotic time, by letting the system cool down after 300 fm/c (where the excitation is around 3.5 MeV per nucleon) through a process of sequential evaporation, simulated in-flight in the swarm of light ejectiles and fragments (for this purpose, the model SIMON [35] was used). In the cold system the fragment multiplicity results increased by secondary decay

¹Nuclear fragments are identified through a coalescence algorithm in phase-space which defines the corresponding mass and charge content. The fragment charge Z and mass A are approximated to integer numbers under the constraint of mass, charge, momentum and energy conservation.

up to around 45 AMeV and levels off for larger bombarding energies due to a more prominent decay into light fragments. The system evolves from a dominance of incomplete fusion around 20 AMeV to a full multifragmentation pattern. This result is in close accordance with experimental observations addressed to the same system, where multifragmentation is already seen above 30 AMeV [34]. On the other hand, if the BLOB approach is replaced by a SMF calculation with corresponding mean-field parameters, the transition moves above 40 AMeV. Hence the formation of inhomogeneities is enhanced in the BLOB approach and, beside a possible additional amplification from spinodal modes, this process is induced by fluctuations which are implemented in full phase space. Hence BLOB is able to reproduce experimental observations related to the onset of multifragmentation better than previous mean-field-based models. Moreover, fluctuations have the effect of anticipating the formation of fragments. Indeed, the fraction of energy spent in light-particle emission reduces in favour of a larger contribution to the developing of inhomogeneities and of a more explosive dynamics, which drives the separation of those inhomogeneities into fragments. This should reflect also in experimental observables like charge and velocity distributions [36]. On the contrary, for small bombarding energies (below 30 AMeV), due to insufficient kinetic energy, the mean field often succeeds to co-

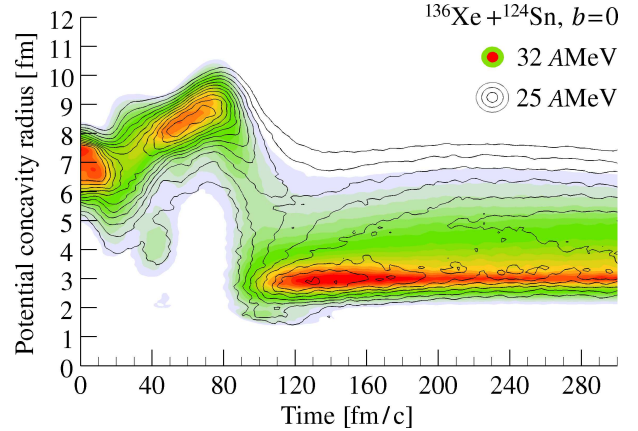


Figure 4: (Color online) Temporal evolution of the size distribution of potential concavities in $^{136}\text{Xe} + ^{124}\text{Sn}$ ($b = 0$) for an incident energy of 32 AMeV (filled contours) and 25 AMeV (contour lines).

alesce all the inhomogeneities or part of them into a compact system.

3.2. Developing of bifurcations

Fluctuations feed the large width of the multiplicity distribution above the multifragmentation threshold. A better insight on their distribution, and on the possible mixing of different reaction mechanisms is provided by the charge asymmetry $\alpha = (Z_1 - Z_2)/(Z_1 + Z_2)$ between the largest fragment Z_1 and the second largest fragment Z_2 , emitted in each event. This observable, presented in fig. 3 illustrates that the reaction mechanism changes from incomplete fusion (charge asymmetry close to unity) to fragmentation (very small charge asymmetry) discontinuously, passing through a bombarding-energy range (around 28 AMeV) where both mechanisms coexist. Thus we observe, at this transition energy, a wide, but discontinuous, bunch of trajectories and a bimodal behaviour of α , indicating that either the system recompacts or it breaks up into several pieces of similar size. Intermediate charge-asymmetry values are never populated. It should be noted that this variety of configurations is related to the same ‘‘macroscopic’’ initial conditions, i.e. the same beam energy and one unique value for the impact parameter. These features, often discussed in the context of the thermodynamics of phase transitions and bimodal behaviour of the order parameter [6, 12, 13], are observed here as a result of the fragmentation dynamics, governed by the spinodal decomposition mechanism. As a consequence of the presence of fluctuations in the dynamical trajectories, the amount of light-particles early emitted may vary from one event to the other, leading to energy fluctuations in the fragmenting system. It follows that this latter behaves as in a thermal bath and, at the transition energy, it oscillates between two configurations which are energetically favourable. The same behaviour is also found in the corresponding SMF approach, but at larger incident energy. After secondary decay, the transition pattern is not washed out if events producing large fission residues are removed, and it could be searched in experimental data relative to the same systems [34].

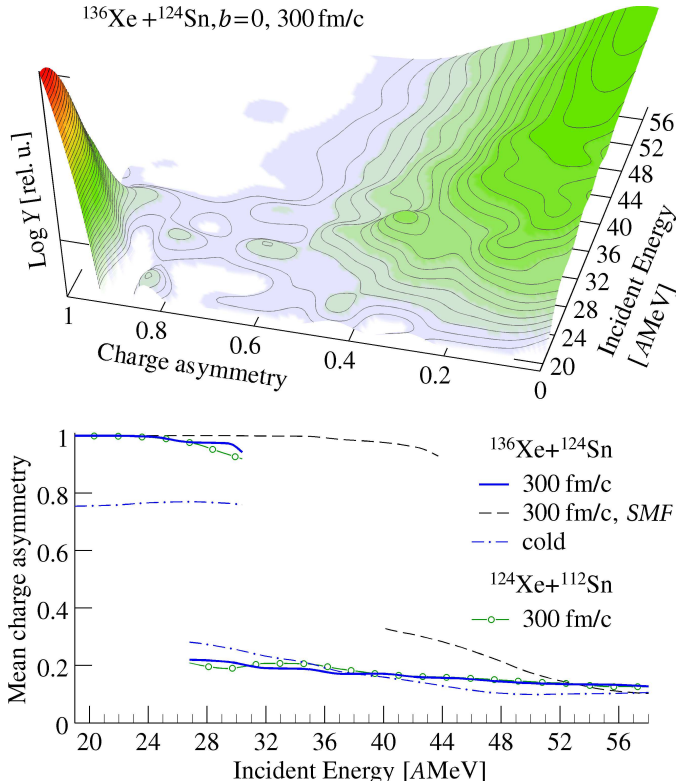


Figure 3: (Color online) Top. Survey of the reaction mechanism: distribution of charge asymmetry α as a function of the incident energy in $^{136}\text{Xe} + ^{124}\text{Sn}$ ($b = 0$) at 300 fm/c. Bottom. Corresponding mean values. Additional calculation for the system $^{124}\text{Xe} + ^{112}\text{Sn}$, and simulation of the heaviest system within the SMF approach and after secondary decay are also displayed.

To explore in finer details the developing of instabilities, the development of concavities in the mean-field potential landscape is followed in time for the incident energies 32 and 25 AMeV. With respect to analysing the fragment features, this analysis has the advantage of applying to earlier times, before fragment formation or when fragments do not appear in the exit channel. The distribution of the corresponding radius is shown in fig. 4. This radius probes the size of forming blobs of matter which are the fragment nesting sites; they may eventually separate into clusters and leave the system (prominent mechanism at 32 AMeV), or merge into larger fragments, or fuse back together forming a large residue (as clearly seen at 25 AMeV). The potential concavity-radius evolves initially with the composite-system size, as marked by the upper branch in fig. 4, and suddenly drops to smaller sizes which characterise all forming droplets of matter within a small variance, as expected for a spinodal multifragmentation picture: this latter defines the lowest branch in fig. 4, and reflects in the bimodal pattern of the charge-asymmetry observable shown in fig. 3.

4. Conclusions and prospects

In conclusion, a promising new framework of transport modelling has been realised by extending the Boltzmann-Vlasov formalism to include a Langevin residual term in the evolution of the one-body distribution function in full phase space and adapted to fermionic systems. This approach reveals to keep the specific character of a one-body theory, as far as the description of mean-field (spinodal) instabilities is concerned, and at the same time to solve the long-standing difficulty of introducing fluctuations of correct amplitude in a Boltzmann formalisation. The model, tested on the transition from fusion to fragmentation in central collisions at Fermi energies, reveals to be closer to the observation than previous attempts to include a Langevin term in Boltzmann theories. Moreover, we have identified the occurrence of bifurcations and bimodal behaviour in dynamical trajectories, linked to the fragment formation mechanism. At the transition energy, the system may either recompact or split into several pieces of similar sizes. We would like to mention that our findings do not challenge the validity of thermodynamical analyses evidencing the occurrence of bimodal behaviour in nuclear fragmentation [12, 13]. Indeed a large fraction of the available phase space is populated through the spinodal decomposition mechanism [8], thus legitimating the use of thermodynamical equilibrium concepts. Our calculations provide a possible explanation, based on the occurrence of dynamical instabilities, of the origin of trajectory bifurcation and bimodality. We found this phenomenology in the bimodal behaviour of quantities related to fragmentation observables in the case of relatively low energies and head-on collisions. As bimodality has not been searched so far in this energy-centrality conditions, the present results are a suggestion for future experimental research.

Finally, we stress that the results presented here may be relevant not only for nuclear fragmentation studies, but in general for the dynamical description of quantum many-body systems.

5. Acknowledgements

Clarifying discussions with M.-F. Rivet, B. Borderie, J. Rizzo and F. Sebille are gratefully acknowledged.

References

- [1] M. Schmidt et al., Phys. Rev. Lett. 86 (2001) 1191; C. Hock et al., Phys. Rev. Lett. 102 (2009) 043401.
- [2] Y.E. Kim and A.L. Zubarev, Phys. Rev. A 70 (2004) 033612.
- [3] J. Steinheimer and J. Randrup, Phys. Rev. Lett. 109 (2012) 212301.
- [4] L.G. Moretto et al., Journal of Physics G 38 (2011) 113101.
- [5] K. Binder and D.P. Landau, Phys. Rev. B 30 (1984) 1477.
- [6] P.Chomaz, V.Duflot, F.Gulminelli, Phys. Rev. Lett. 85 (2000) 3587; P.Chomaz, F.Gulminelli, Physica A 330 (2003) 451.
- [7] D.R. Bowman, G.F. Peaslee, R.T. DeSouza, et al. Phys. Rev. Lett. 67 (1991) 1527.
- [8] B. Borderie, M.F. Rivet, Progr. in Part. and Nucl. Phys. 61 (Book Series) (2008) 551, and refs. therein.
- [9] M. D'Agostino et al., Phys. Lett. B473 (2000) 219.
- [10] H.R. Jaqaman, A.Z. Mekjian, L. Zamick, Phys. Rev. C 27 (1983) 2782.
- [11] H. Müller and B.D. Serot Phys. Rev. C 52 (1995) 2072.
- [12] E.Bonnet et al. (INDRA coll.), Phys. Rev. Lett. 103 (2009) 072701.
- [13] M. Pichon et al. (INDRA coll.), Nucl. Phys. A779 (2006) 267.
- [14] J. Aichelin, Phys. Rep. 202 (1991) 233; A. Bohnet et al., Phys. Rev. C 44 (1991) 2111.
- [15] K. Morawetz, New Journal of Phys. 9 (2007) 313; P. Lipavský, K. Morawetz and V. Špička, Ann. Phys. 26 (2001) 1.
- [16] M.Colonna, A.Ono, J.Rizzo, Phys. Rev. C82 (2010) 054613, and references therein.
- [17] Ph. Chomaz, M. Colonna and J. Randrup, Phys. Rep. 389 (2004) 263.
- [18] A. Le Fèvre et al., Phys. Rev C 80 (2009) 044615.
- [19] Y. Abe, S. Ayik, P.-G. Reinhard, and E. Suraud, Phys. Rep. 275 (1996) 49.
- [20] D. Lacroix, S. Ayik, and B. Yilmaz, Phys. Rev. C 85 (2012) 041602(R).
- [21] S. Ayik and C. Grégoire, Nucl. Phys. A513 (1990) 187.
- [22] J. Randrup and B. Remaud, Nucl. Phys. A514 (1990) 339.
- [23] G.F. Burgio, Ph. Chomaz and J. Randrup, Nucl. Phys. A529 (1991) 157.
- [24] M. Colonna et al. Nucl. Phys. A642 (1998) 449.
- [25] G.F. Bertsch and S. Das Gupta, Phys. Rep. 160 (1988) 189.
- [26] J. Rizzo, Ph. Chomaz and M. Colonna, Nucl. Phys. A806 (2008) 40.
- [27] W. Bauer, G.F. Bertsch and S. Das Gupta, Phys. Rev. Lett. 58 (1987) 863.
- [28] F. Chapelle, G.F. Burgio, Ph. Chomaz and J. Randrup, Nucl. Phys. A540 (1992) 227.
- [29] P.G. Reinhard, E. Suraud Annals of Physics 216 (1992) 98.
- [30] P. Napolitani and M. Colonna, EPJ Web of Conf. 31 (2012) 00027, IWM2011.
- [31] M. Colonna and Ph. Chomaz, Phys. Rev. C 49 (1994) 1908.
- [32] V. Baran, M. Colonna, V. Greco and M. Di Toro, Phys. Rep. 410 (2005) 335.
- [33] P.Danielewicz, Acta Phys.Polon. B33 (2002) 45; D.D.S. Coupland, W.G. Lynch, M.B. Tsang, P. Danielewicz and Y. Zhang, Phys. Rev C 84 (2011) 054603.
- [34] F. Gagnon-Moisan et al. (INDRA coll.), Phys. Rev C 86 (2012) 044617.
- [35] D. Durand, Nucl. Phys. A541 (1992) 266.
- [36] P. Napolitani et al., in preparation.